HTML ABSTRACT + LINKS

Short-period intrinsic Stark GaN/AlGaN superlattice as a Bloch oscillator

V. I. Litvinov[a)]
WaveBand Corporation, 17152 Armstrong Avenue, Irvine, California 92614

A. Manasson and D. Pavlidis
University of Michigan, Department of Electrical Engineering and Computer Science, 1301 Beal Avenue, Ann Arbor, Michigan 48109

(Received 1 March 2004; accepted 27 May 2004)

We discuss the properties of AlGaN/GaN superlattice (SL) related to the feasibility of a terahertz-range oscillator. The distortion of the conduction-band profile by the polarization fields has been taken into account. We have calculated the conduction-band offset between the pseudomorphic AlGaN barrier and the GaN quantum well, the first miniband width and energy dispersion, as functions of Al content in the barrier. As the short-period SL miniband energy dispersion contains contributions from next to nearest neighbors, it causes anharmonic electron oscillations at the multiples of the fundamental Bloch frequency. The Al content and SL period that favor high-frequency oscillations have been determined. © *2004 American Institute of Physics*.
[DOI: 10.1063/1.1773913]

Negative differential conductivity (NDC) in semiconductor superlattices (SLs)[1] is at the origin of various proposals for compact submillimeter wave sources. The NDC in dc-biased SLs results in traveling electrical domain formation that has been used in a 147 GHz microwave source made of the InGaAs/GaAs SL.[2,3] Another type of SL source, the Bloch oscillator,[1] is projected to oscillate at the Bloch frequency (terahertz region) and exploits the existence of high-frequency NDC. At the moment, no live example of the Bloch-type source exists because the NDC at zero frequency induces electric-field domains, thus preventing electrons from oscillating at the Bloch frequency.[4,5] Operation of the SL source relies on carrier dynamics specific to a narrow conduction band. High-frequency and zero-frequency NDC may or may not appear simultaneously depending on details of the miniband electron energy dispersion. If the dispersion is not of simple cosine-type, it is possible to arrange the high-frequency NDC while suppressing the dc instability. This prevents electrical domain formation and allows Bloch oscillations.

The output power of the source depends on the current and voltage swing in the NDC region. Basically, it would be beneficial to high-power device operation if the SL structure was made of a wide band-gap semiconductor. Thus, the GaN/AlGaN SL is a possible candidate for high-power submillimeter wave source. GaN-based electronic devices can sustain higher voltage and are less sensitive to the high dislocation density as compared to narrow-gap GaAs–InAs-based devices.

In this letter, we discuss the properties of an AlGaN/GaN SL relevant to microwave source feasibility. The wurtzite (0001)AlGaN/GaN SL is the intrinsic Stark SL where the polarization fields shift the energy levels of confined electrons. Proper design of a GaN/AlGaN SL source should account for intrinsic electric fields. Polarization fields in a SL stem from the spontaneous polarization in the bulk and lattice-mismatch-induced piezoelectric component. We calculate the electron energy dispersion and width of the first miniband in the intrinsic Stark GaN-based SL and discuss the results related to feasibility of a submillimeter wave source.

The dynamic properties of the SL depend on the conduction-band profile as determined by the conduction-band offset. We assume that the band gap in the relaxed $Al_xGa_{1-x}N$ alloy layer is described as follows:

$$E_g^0(x)=xE_g^{\mathrm{AlN}}+(1-x)E_g^{\mathrm{GaN}}-bx(1-x), \tag{1}$$

where $E_g^{\mathrm{AlN}}=6.2$ eV, $E_g^{\mathrm{GaN}}=3.42$ eV, and the bowing parameter $b=1$ eV, x is the Al composition of the alloy. We use linear interpolations to calculate the electron effective mass m, (in units of free electron mass) and the lattice parameter a in the basal plane of the alloy:

$$m(x)=xm_{\mathrm{AlN}}+(1-x)m_{\mathrm{GaN}};\ \ m_{\mathrm{AlN}}=0.27,\ \ m_{\mathrm{GaN}}=0.2,$$

$$a(x)=xa_{\mathrm{AlN}}+(1-x)a_{\mathrm{GaN}};\ \ a_{\mathrm{AlN}}=3.11A,\ \ a_{\mathrm{GaN}}=3.19A. \tag{2}$$

In-plane tensile strain in thin (pseudomorphic) AlGaN barriers is given as

$$\zeta(x)=\frac{a_{\mathrm{GaN}}-a(x)}{a(x)}. \tag{3}$$

The band edge positions in the AlGaN layers are given below with the reference energy taken at the valence-band edge of the relaxed layer. The position of the conduction $C(x)$ and valence $V(x)$ bands are given as

$$C(x)=E_g(x)+3A_c\zeta(x),$$

$$V(x)=2\zeta(x)\left[(D_2+D_4)-(D_1+D_3)\frac{C_{13}(x)}{C_{33}(x)}\right], \tag{4}$$

$$C_{13}(x)=(5x+103);\ \ C_{33}(x)=(-32x+405),$$

where the deformation potentials are given in eV and the elastic constants in GPa:[6] $A_c=-4.6$, $D_1=-1.7$, $D_2=6.3$, $D_3=8$, and $D_4=-4$, respectively. We assume that deformation potentials are independent of the Al content x.

a)Electronic mail: vlitvinov@waveband.com

 © 2004 American Institute of Physics

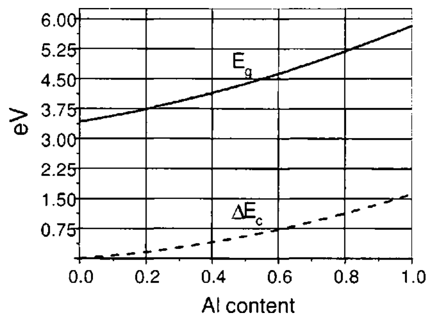

FIG. 1. The band gap in tensiled AlGaN barrier and the conduction-band offset as functions of Al content.

Using Eqs. (1)–(4), the strained layer band gap, i.e., the energy difference between conduction and heavy hole band edges, is given by

$$E_g(x) = C(x) - V(x) \approx 3.42 + 1.39x + x^2. \quad (5)$$

The natural valence-band offset ΔE_v between AlN and GaN is 0.8 eV.[7] Assuming linear interpolation between AlGaN and GaN binary ends, $\Delta E_v(x)=0.8x$ eV, the conduction-band offset is found as follows:

$$\Delta E_c(x) = E_g(x) - E_g^{\mathrm{GaN}} - \Delta E_v(x) \approx 0.603x + 0.99x^2 \ [\mathrm{eV}]. \quad (6)$$

The band gap and conduction-band offset are shown in Fig. 1 as functions of Al content.

Built-in electric fields in a SL, caused by spontaneous and piezoelectric polarizations, can be calculated using the following equations:

$$F_{\mathrm{well}} = \frac{P_{\mathrm{total}} d_b}{\varepsilon_0[\varepsilon(x)d_w + \varepsilon(0)d_b]}, \quad F_{\mathrm{barrier}} = -\frac{P_{\mathrm{total}} d_w}{\varepsilon_0[\varepsilon(x)d_w + \varepsilon(0)d_b]}, \quad (7)$$

where the polarization is given as

$$P_{\mathrm{total}}(x) = P_{\mathrm{sp}}(0) - P_{\mathrm{sp}}(x) - 2\zeta(x)\left[e_{31} + e_{33}\frac{C_{13}(x)}{C_{33}(x)}\right], \quad (8)$$

where $P_{\mathrm{sp}}(x)=(-0.052x-0.029)\ \mathrm{C/m^2}$ is the spontaneous polarization in $\mathrm{Al}_x\mathrm{Ga}_{1-x}\mathrm{N}$ alloy; $e_{31}=0.3$, $e_{33}=1$ are GaN piezoelectric constants $(\mathrm{C/m^2})$, $\varepsilon(x)$ is the dielectric constant of AlGaN, d_b, d_w are thicknesses of barrier and well, respectively, and $d=d_w+d_b$ is the SL period. The resulting conduction band profile including polarization effects is shown in Fig. 2.

The analytically obtained profile from Eqs. (6) and (7), shown in Fig. 2, was confirmed by numerical calculations with help of the Poisson–Schrödinger solver. Solver-based calculations account for polarization fields by including delta-doped regions that simulate polarization charges at the interfaces.

The first mininband width in InGaN/AlGaN/GaN SLs calculated in Ref. 8 does not account for polarization fields in the structure. In this letter, the miniband energy dispersion in the polarization-distorted band profile was calculated within the tight-binding approximation:

$$\varepsilon(k) - \varepsilon_0 = \frac{\sum_n h(n)\exp(iknd)}{\sum_n I(n)\exp(iknd)}, \quad (9)$$

where

$$h(n) = \int \varphi^*(z)h(z)\varphi(z-nd)dz;$$
$$I(n) = \int \varphi^*(z)\varphi(z-nd)dz, \quad (10)$$

where $h(n)$ is the hopping integral, and $\varphi(z)$ is the wave function of a single SL period shown in Fig. 3. The wave function in Fig. 3 was calculated by solving Schrödinger equation with the potential also shown in Fig. 3.

An electron energy dispersion curve is shown in Fig. 4 (solid line). It should be noted that in the range of compositions $(0.18<x<0.4)$ and SL periods $d<50$ Å, the calculation of the miniband energy dispersion requires more than first-nearest-neighbor terms in the dispersion law. Figure 4 illustrates the difference between results obtained using only nearest-neighbors and high-order terms.

The electron energy dispersion in the first miniband, shown in Fig. 4 (solid line), has more complex behavior than the simple cosine-law normally used in the kinetic equation to study electron dynamics in a narrow band. The reason

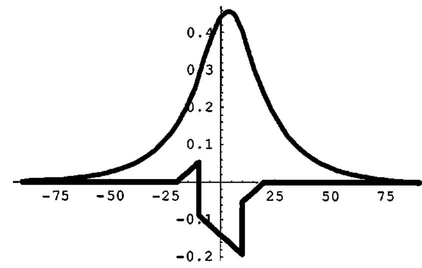

FIG. 3. The single-period potential (eV) and electron wave function (a.u.) as functions of a distance from the well (Å); $x=0.18$ and $d_w=20$ Å.

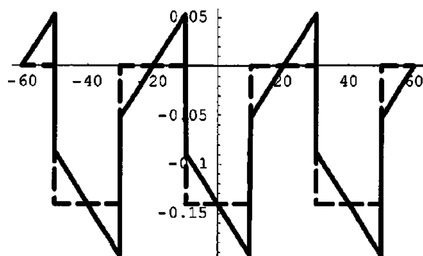

FIG. 2. Conduction-band profile in AlGaN/GaN SL (eV) in growth direction (Å): Solid line—polarization fields included; dashed line—flat-band approximation; $x=0.18$ and $d_b=d_w=20$ Å.

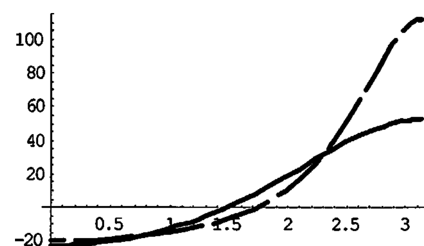

FIG. 4. First miniband energy dispersion (meV) as a function of kd; $x=0.18$ and $d_b=d_w=20$ Å; solid line—four nearest-neighbor approximation; dashed line—first-nearest-neighbor approximation.

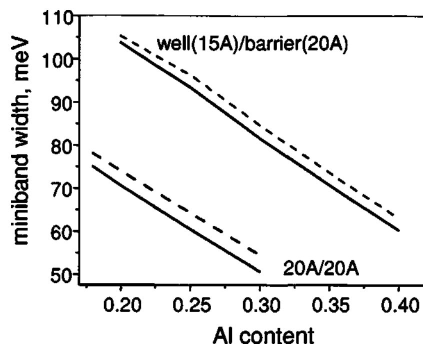

FIG. 5. First miniband width in AlGaN/GaN SL: Dashed line—flat-band approximation; solid line—polarization fields included.

behind that is the large spatial size of the single-period wave function as compared to the SL period. The calculated miniband width is shown in Fig. 5.

To verify the validity of the tight-binding approach in short-period SLs, we have studied the 11.7 A thick AlAs-barrier/36.3 A-thick GaAs-well SL and obtained good agreement with the experimentally confirmed miniband width.[9] In addition, our results agree well with those obtained with the Kronig–Penney calculations[10] when a flat-band approximation is assumed. The reason we use the tight-binding approach instead of the Kronig–Penney approach is that the former easily allows one to include polarization fields into the scheme. Also, the tight-binding scheme in short-period SLs has already been used[11–13] and experimentally justified in Refs. 11 and 12. Next-to-nearest-neighbor generalization within the tight-binding approach was considered in Ref. 13 with respect to electron dynamic localization and oscillations in biased SLs.

In conclusion, we have found a miniband energy dispersion in the AlGaN/GaN SL. The result accounts for spontaneous and strain-induced polarizations. Miniband width is calculated as functions of the Al composition and layer thickness. It is shown that the short-period AlGaN/GaN SL $(0.18 < x < 0.4; d < 50\ \text{Å})$, may provide conditions for the anharmonic electron oscillations at integer multiples of the fundamental Bloch frequency, thus providing the dc-electric-field regions where dynamic NDC is negative while the dc instability is suppressed.

The authors acknowledge financial support from Air Force STTR program under the direction of Dr. Gernot Pomrenke.

[1] L. Esaki and R. Tsu, IBM J. Res. Dev. **14**, 61 (1970).
[2] E. Schomburg, R. Scheuerer, S. Brandl, K. F. Renk, D. G. Pavel'ev, Y. Koschurinov, V. Ustinov, A. Zhukov, A. Kovsch, and P. S. Kop'ev, Electron. Lett. **35**, 1491 (1999).
[3] Schomburg, S. Brandl, K. Hofbeck, T. Bloemeier, J. Grenzer, A. A. Ignatov, K. F. Renk, D. G. Pavel'ev, Y. Koschurinov, V. Ustinov, A. Zhukov, A. Kovsch, S. Ivanov, and P. S. Kop'ev, Appl. Phys. Lett. **72**, 1498 (1998).
[4] H. Kroemer, cond-mat/0009311 (2000).
[5] Y. Romanov and Y. Y. Romanova, Phys. Solid State **46**, 164 (2003); Y. Romanov, L. G. Murokh, and N. J. M. Horing, J. Appl. Phys. **93**, 4696 (2003).
[6] M. Kumagai, S. L. Chuang, and H. Ando, Phys. Rev. B **57**, 15303 (1998).
[7] H. Wei and A. Zunger, Appl. Phys. Lett. **72**, 2011 (1998).
[8] V. I. Litvinov, V. A. Manasson, and L. Sadovnik, Proc. SPIE **4111**, 116 (2000).
[9] S. Winnerl, E. Schomburg, J. Grenzer, H. J. Regl, A. A. Ignatov, A. D. Semenov, K. F. Renk, D. G. Pavel'ev, Yu. Koschurinov, B. Melzer, V. Ustinov, S. Ivanov, S. Schaposchinikov, and P. S. Kop'ev, Phys. Rev. B **56**, 10303 (1997).
[10] G. Bastard, *Wave mechanics applied to semiconductor heterostructures* (Halsted, New York, 1988).
[11] P. Boring, J. M. Jancu, B. Gil, D. Bertho, C. Jouanin, and K. J. Moore, Phys. Rev. B **46**, 4764 (1992).
[12] A. B. Henriques, Phys. Rev. B **50**, 8658 (1994).
[13] A. W. Ghosh and J. Wilkins, Phys. Rev. B **61**, 5423 (2000).